

# Reaction mechanisms in massive nuclei collisions and perspectives for synthesis of heavier superheavy elements

GIARDINA G<sup>1,2,\*</sup> NASIROV A K<sup>3,4</sup> MANDAGLIO G<sup>1,2,5</sup> CURCIARELLO F<sup>1,2</sup>  
De LEO V<sup>1,2</sup> FAZIO G<sup>1,2</sup> ROMANIUK M<sup>1,2</sup>

<sup>1</sup>*Dipartimento di Fisica e di Scienze della Terra dell'Università di Messina, Messina 98166, Italy*

<sup>2</sup>*Istituto Nazionale di Fisica Nucleare, Sezione di Catania, Catania 95123, Italy*

<sup>3</sup>*Joint Institute for Nuclear Research, Dubna 141980, Russia*

<sup>4</sup>*Institute of Nuclear Physics, Tashkent 100214, Uzbekistan*

<sup>5</sup>*Centro Siciliano di Fisica Nucleare e Struttura della Materia, Catania 95125, Italy*

**Abstract** We discuss a hardship in synthesis of heaviest super heavy elements in massive nuclei reactions due to the hindrance to complete fusion of reacting nuclei caused on the onset of quasifission process which strongly competes with complete fusion and due to the strong increase of fission yields along the de-excitation cascade of the compound nucleus in comparison with the evaporation residue formation. The hindrance to formation of compound nucleus and evaporation residue is determined by the characteristic of the entrance channel.

**Key words** Capture, Quasifission, Complete fusion, Fast fission, Fusion-fission, Evaporation residue

## 1 Introduction

In massive nuclei collisions, reactions evolve through various steps and different processes which determine the nature and characteristics of reaction products in dependence of the choice and conditions of reacting nuclei in the entrance channel. Therefore, different reactants which reach the same compound nucleus (CN)-characterized by the same mass number  $A$ , atomic number  $Z$ , and excitation energy  $E_{\text{CN}}^*$  do not lead to the same reaction products with the same dynamical characteristics<sup>[1-3]</sup>. Compound nuclei formed by very different entrance channels are characterized by different angular momentum distributions at the same  $E_{\text{CN}}^*$ . In this context, a very mass asymmetric reaction in the entrance channel, for which a dinuclear system (DNS) is formed after capture of reactants, mainly evolves to complete fusion (CF) and reaches the stage of CN. Then, the de-excitation behavior of CN is determined by competition between fission and particle evaporation processes. Instead, the DNS formed in a more mass

symmetric reaction in the entrance channel, undergoes strong hindrance in its evolution to CN due to the competition with the quasifission process (QF) which is the decay of DNS into two fragments. In this case, the QF yield increases and the CF rate decreases by increasing the mass and charge of nuclei in the entrance channel. Consequently, in some cases the evaporation residue (ER) cross section  $\sigma_{\text{ER}}$  decreases reaching values lower than 1 pb. To prove the above-mentioned statements we consider as examples of entrance channels the following reactions:  $^{22}\text{Ne}+^{248}\text{Cf}$  (very mass asymmetric reaction),  $^{24}\text{Mg}+^{248}\text{Cm}$ ,  $^{34}\text{S}+^{238}\text{U}$  (less mass asymmetric reaction),  $^{40}\text{Ar}+^{232}\text{Th}$  (more mass symmetric reaction),  $^{132}\text{Sn}+^{140}\text{Ce}$  (almost mass symmetric reaction), and  $^{136}\text{Xe}+^{136}\text{Xe}$  (mass symmetric reaction) leading to the same  $^{272}\text{Hs}$  CN. In the case of the  $^{22}\text{Ne}$  induced reaction the capture cross section is mainly transformed in complete fusion cross section at low energy beam<sup>[3]</sup>, and the subsequent ER formation is the dominant part of reaction products. At higher energies besides of the large contribution of QF, the FF formation competes with the ER yields at

\* Corresponding author. E-mail address: ggiardina@unime.it

Received date: 2013-06-27

de-excitation of CN. In the case of the  $^{34}\text{S}$  induced reaction, the QF cross section is at least one order of magnitude higher than the CN cross section because the CF is strongly hindered by the dominant role of QF, and at decay of CN the fission rate is higher than the ER process<sup>[4]</sup>. In the case of the  $^{40}\text{Ar}$  induced reaction the  $\sigma_{\text{ER}}$  formation is lower than 1 pb. This result is jointly caused by the dominant role of QF in comparison to fusion, and to the dominant role of the fission process in comparison to the evaporation one. Moreover, in the cases of the  $^{132}\text{Sn}+^{140}\text{Ce}$  and  $^{136}\text{Xe}+^{136}\text{Xe}$  reactions the ER formation completely disappears.

The competition between QF and CF processes depends on the orbital angular momentum distribution of DNS. Consequently, also the formation of the rotating and excited CN is characterized by the mass asymmetry of reactants in the entrance channel through a specific angular momentum distribution of DNS. Therefore, the same CN, which is formed by different entrance channels, characterized by the same  $E_{\text{CN}}^*$  has different angular momentum distributions. Certainly, it decays differently in competition between processes forming fission fragments (FF) or evaporation residue nuclei (ERs), along the various steps of the de-excitation cascade. Since the fission barriers (contributed by macroscopic and microscopic parts of nuclear binding energy) of CN and intermediate excited nuclei are dependent on the nuclear temperature  $T$  and angular momentum  $\ell$ , the rates of fission fragments and ERs are sensitive to the specific dynamical properties of CN and intermediate excited nuclei determined by the used reactants in the entrance channel. Therefore, the ER cross sections decrease by increasing the angular momentum due to its influence on the rotating CN. Finally, the CN formed at the same  $E_{\text{CN}}^*$  by different entrance channels decays forming products (FFs and ERs) with different properties because the CN retains the dynamic peculiarities of reacting nuclei in the entrance channel. In order to give realistic estimations of the reaction product cross sections by mass symmetric or almost symmetric reactants as entrance channel, an adequate model which allows one to describe by a reliable way the complex dynamics of mechanisms

during all stages of reaction has to be developed. In fact, in the last stage of nuclear reaction, the formed CN may de-excite by fission (producing fusion-fission fragments) or by emission of light particles. The reaction products that survive fission are ERs. The registration of ER is a clear evidence of the CN formation, but in case of reactions with massive nuclei, generally, the knowledge of the ERs formation only is not enough to determine the complete fusion cross section and to understand the dynamics of the de-excitation cascade of CN if the true fission fragments are not correctly taken into account. On the other hand, the correct identification of an evaporation residue nucleus by the observation of its decay chain does not assure if the target material contains other isotopes of the nucleus under consideration. In fact, for example, in the case of the  $^{48}\text{Ca}+^{249}\text{Cf}$  reaction, the identification of the  $^{294}118$  nucleus as the evaporation residue of the  $^{297}118$  CN after the emission of 3 neutrons (see the experiment reported in Ref.[5]) cannot assure that the collected events corresponding to the  $^{294}118$  nucleus are obtained only due to the mentioned reaction leading to the formation of the  $^{297}118$  CN. The interaction of the  $^{48}\text{Ca}$  projectile with the  $^{250}\text{Cf}$  isotope in target should be considered in order to take into account the contribution of the  $^{48}\text{Ca}+^{250}\text{Cf}$  reaction to the  $^{294}118$  ER formation because the target material inevitably contains the  $^{250}\text{Cf}$  isotope too. In fact, in this last case, the  $^{48}\text{Ca}+^{250}\text{Cf}$  reaction (forming the  $^{298}118$  CN) leads to the same  $^{294}118$  evaporation residue nucleus after emission of 4 neutrons from CN. This effect depends on the  $E_{\text{CN}}^*$  excitation energy of CN which is determined by the collision energy  $E_{\text{c.m.}}$ . In addition, the use of some assumptions about the reaction mechanisms leading to the formation of the observed fission-like fragments, does not allow for sure correct determination of the fusion-fission contribution in the case of overlapping of the mass fragment distributions due to different processes (quasifission, fast fission and fusion-fission)<sup>[1,3,6,7]</sup>. The exigency and importance to have a multiparameter and sensitive model is strongly connected with the requirement to reach reliable results and with the possibility to give

reliable estimations of perspectives for the synthesis of superheavy elements (SHE).

## 2 Model and formalism

By using the DNS model<sup>[8]</sup>, the first stage of reaction is the capture formation of a DNS after full momentum transfer of the relative motion of colliding nuclei into a rotating and excited nuclear system. In the deep inelastic collisions DNS is formed but the full momentum transfer does not occur. Therefore, the deep inelastic collisions are not capture reactions.

The partial capture cross section at a given energy  $E_{c.m.}$  and orbital angular momentum  $\ell$  is determined by Eq.(1).

$$\sigma_{cap}^{\ell}(E_{c.m.}) = \pi \lambda^2 P_{cap}^{\ell}(E_{c.m.}) \quad (1)$$

where the capture probability  $P_{cap}^{\ell}(E_{c.m.})$ —equal to 1 or 0 for a given  $E_{c.m.}$  energy and orbital angular momentum  $\ell$  in dependence on the result of dynamical calculations—is the path of collision trapped into the nucleus-nucleus potential well or not, respectively, after dissipation of part of the initial relative kinetic energy and orbital angular momentum<sup>[1,9]</sup>. Our calculations showed that, depending on the center-of-mass system energy  $E_{c.m.}$ , there can be “window” in the orbital angular momentum for capture with respect to the conditions described in Refs.[1,9]. The quasifission process competes with formation of CN. This process occurs when the DNS prefers to break down into two fragments instead of transforming into the fully equilibrated CN. The fusion excitation function is determined by product of the partial capture cross section  $\sigma_{cap}^{\ell}$  and the fusion probability  $P_{CN}$  of DNS, at various  $E_{c.m.}$  values:

$$\sigma_{fus}(E_{c.m.}; \beta_p, \alpha_T) = \sum_{\ell=0}^{\ell_f} (2\ell+1) \times \sigma_{cap}(E_{c.m.}; \ell, \beta_p, \alpha_T) P_{CN}(E_{c.m.}; \ell, \beta_p, \alpha_T). \quad (2)$$

Obviously, the quasifission cross section is defined by

$$\sigma_{qfis}(E_{c.m.}; \beta_p, \alpha_T) = \sum_{\ell=0}^{\ell_f} (2\ell+1) \times \sigma_{cap}(E_{c.m.}; \ell, \beta_p, \alpha_T) (1 - P_{CN}(E_{c.m.}; \ell, \beta_p, \alpha_T)). \quad (3)$$

For more specific details and descriptions of the model see Refs.[1,7,9-11]. In order to show the sensitivity of our model, we present in Fig.1 the calculated  $P_{CN}$  fusion probability as a function of the orbital angular

momentum  $\ell$ , at excitation energies  $E_{CN}^* = 49$  MeV (dashed line) and 63 MeV (full line) of the  $^{202}\text{Pb}$  CN in the  $^{48}\text{Ca} + ^{154}\text{Sm}$  reaction.

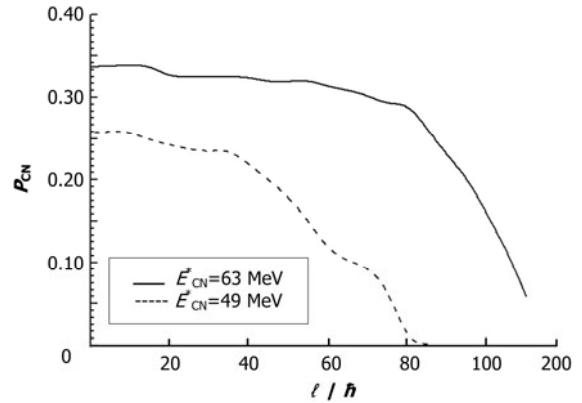


**Fig.1** The  $P_{CN}$  fusion probability calculation vs. the orbital angular momentum  $\ell$  for the  $^{48}\text{Ca} + ^{154}\text{Sm}$  reaction, at two different  $E_{CN}^*$  values of the  $^{202}\text{Pb}$  CN.

Figure 1 shows how much the  $P_{CN}$  fusion probability changes with the  $\ell$  value at a fixed  $E_{CN}^*$  excitation energy of CN, and how much the  $P_{CN}$  trend of changes at two different  $E_{CN}^*$  values. Therefore, the methods that do not take into account in calculation the dependence of the  $P_{CN}$  fusion probability on the collision energy  $E_{c.m.}$ , angular momentum  $\ell$ , and on the orientation angles of the axial symmetry axes of deformed reacting nuclei cannot reach reliable values of the fusion cross section.

The fast fission cross section is calculated by summing the contributions of the partial waves corresponding to the range  $\ell_f \leq \ell \leq \ell_d$  leading to the formation of a mononucleus where the fission barrier  $B_f$  is zero<sup>[7]</sup> in such range of  $\ell$ , and therefore the system promptly decays into two fragments:

$$\sigma_{fastfis}(E_{c.m.}; \beta_p, \alpha_T) = \sum_{\ell=\ell_f}^{\ell_d} (2\ell+1) \times \sigma_{cap}(E_{c.m.}; \ell, \beta_p, \alpha_T) (P_{CN}(E_{c.m.}; \ell, \beta_p, \alpha_T)). \quad (4)$$

The capture cross section is equal to the sum of the quasifission, fusion, and fast fission cross sections<sup>[6]</sup>:

$$\sigma_{cap}^{\ell}(E_{c.m.}; \beta_p, \alpha_T) = \sigma_{qfis}^{\ell}(E_{c.m.}; \beta_p, \alpha_T) + \sigma_{fus}^{\ell}(E_{c.m.}; \beta_p, \alpha_T) + \sigma_{fastfis}^{\ell}(E_{c.m.}; \beta_p, \alpha_T). \quad (5)$$

It is clear that the fusion cross section includes the cross sections of evaporation residues and fusion-fission products<sup>[7]</sup>. The ER cross section is

calculated by the advanced statistical code<sup>[12-14]</sup> that takes into account the damping of the shell correction in the fission barrier as a function of nuclear temperature and orbital angular momentum in determination of the survival probability

$$\sigma_{\text{ER}(x)}(E_x^*) = \sum_{\ell=0}^{\ell_d} (2\ell+1) \sigma_{(x-1)}^{\ell}(E_x^*) W_{\text{sur}(x-1)}(E_x^*, \ell). \quad (6)$$

We are able to calculate mass- and angle-distribution of quasifission and fusion-fission fragments, anisotropy of the fission fragment angular distribution and the dependence of cross sections, Coulomb barrier, intrinsic fusion barrier and quasifission barrier as a function of the orientation angle of the symmetry axes of colliding nuclei (see Refs.[3,7,15]). In Fig.2 we present, as an example, the mass distribution of quasifission fragments for the  $^{48}\text{Ca}+^{154}\text{Sm}$  reaction.

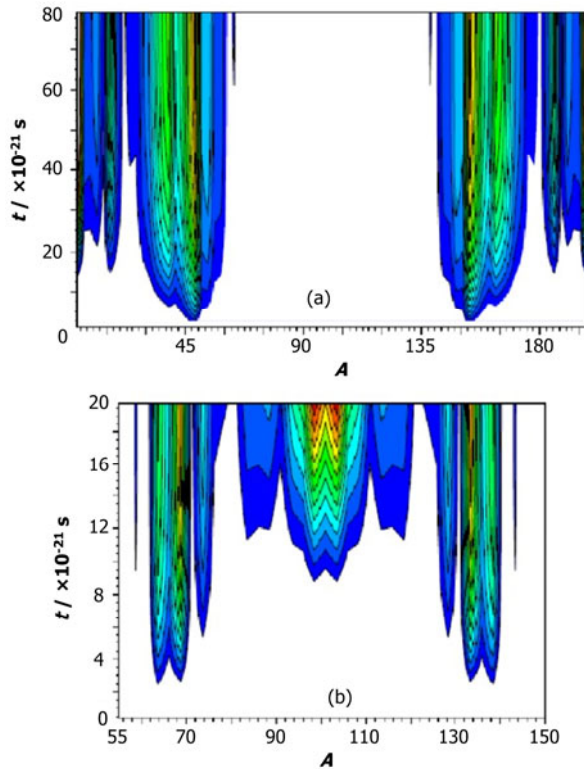


**Fig.2** (Color online) (a) Mass distributions of the quasifission products yield in the  $^{48}\text{Ca}+^{154}\text{Sm}$  reaction at  $E_{\text{c.m.}}=140$  MeV as a function of the lifetime of the dinuclear system formed at capture stage. (b) Mass distributions of the quasifission product yields in the  $^{48}\text{Ca}+^{154}\text{Sm}$  reaction at  $E_{\text{c.m.}}=160$  MeV as a function of the lifetime of the dinuclear system.

In many cases, in dependence on the entrance channel peculiarities, the mass distributions of the fusion-fission, quasifission, and fast fission fragments can overlap<sup>[3,10]</sup>. As a result, the real difficulties arise

in the analysis of experimental data in order to identify the true yields of fragments according to corresponding processes in heavy-ion collisions. Fig.2 shows that at lower  $E_{\text{c.m.}}$  energy the mass distribution of quasifission products populates the asymmetric mass region at any lifetime value of DNS (Fig.2a), while at higher  $E_{\text{c.m.}}$  energy it is also populated the symmetric mass region for longer DNS lifetimes (Fig.2b). The lifetime, in fact, of an excited DNS for a given reaction depends on the initial collision energy  $E_{\text{c.m.}}$  and angular momentum distribution values. Therefore, the DNS during its evolution can evolve to complete fusion (fusion process) or can decay into two fragments (quasifission process).

The competition between these two processes is related to the values of intrinsic fusion barrier  $B_{\text{fus}}^*$  and quasifission barrier  $B_{\text{qf}}$ <sup>[1,2,16]</sup> depending on the peculiarities of reacting nuclei, beam energy and angular momentum distribution.

### 3 Comparison between the $^{136}\text{Xe}+^{136}\text{Xe}$ and $^{24}\text{Mg}+^{248}\text{Cm}$ reactions leading to $^{272}\text{Hs}$ CN

In order to check if any projectile and target combination can always lead to the complete fusion of reactants (having an enough high energy beam to overcome the Coulomb barrier) and synthesis of the wanted SHE, we consider the case of the  $^{136}\text{Xe}+^{136}\text{Xe}$  mass symmetric reaction which would lead to the  $^{272}\text{Hs}$  CN. By using the procedure presented in the previous Section, for this reaction, the results are shown in Fig.3. Fig.3a shows the capture, quasifission, fusion and fast fission cross sections vs.  $E_{\text{c.m.}}$  energy. And Fig.3b shows the fusion probability  $P_{\text{CN}}$  in the same explored  $E_{\text{c.m.}}$  energy range. As one can see the capture cross section for the  $^{136}\text{Xe}+^{136}\text{Xe}$  reaction is about 10 mb in the explored energy range while the fusion cross section leading to the  $^{272}\text{Hs}$  CN ranges between  $10^{-4}$  and  $10^{-1}$  pb (with a fusion probability of about  $10^{-14}$ – $10^{-11}$ ) in the same  $E_{\text{c.m.}}$  interval. By the present investigation we can conclude that the evaporation residue cross section is much lower than  $10^{-10}$  pb. Such a value practically means that no synthesis event of reacting nuclei occurs.

For a comparison with the results for the last reaction, as shown in Fig.4(a), the results obtained in

this work for the mass asymmetric  $^{24}\text{Mg}+^{248}\text{Cm}$  reaction leading to the same  $^{272}\text{Hs}$  CN, where in lower-medium  $E_{\text{c.m.}}$  energy range, the fusion process is dominated in the reaction dynamics. At high energy, the quasifission process prevails. Fig.4(b) shows the ER cross sections. From the comparison of the results presented in Figs.3 and 4, we can conclude that the fusion-fission cross section in the  $^{24}\text{Mg}+^{248}\text{Cm}$  reaction at  $E_{\text{CN}}^*$  of about 55 MeV ( $E_{\text{c.m.}}=192$  MeV) is about 150 mb, while the results for the above-mentioned fusion-fission cross section with the mass symmetric distribution in the  $^{136}\text{Xe}+^{136}\text{Xe}$  reaction is lower than some pb (because the reaction dynamics is completely dominated by the quasifission process). For this symmetric reaction, the fusion-fission yield is at the same  $E_{\text{CN}}^*$  excitation energy of 55 MeV ( $E_{\text{c.m.}}=355$  MeV), at least  $10^{-12}$  times lower than the one obtained by the  $^{24}\text{Mg}+^{248}\text{Cm}$  reaction.

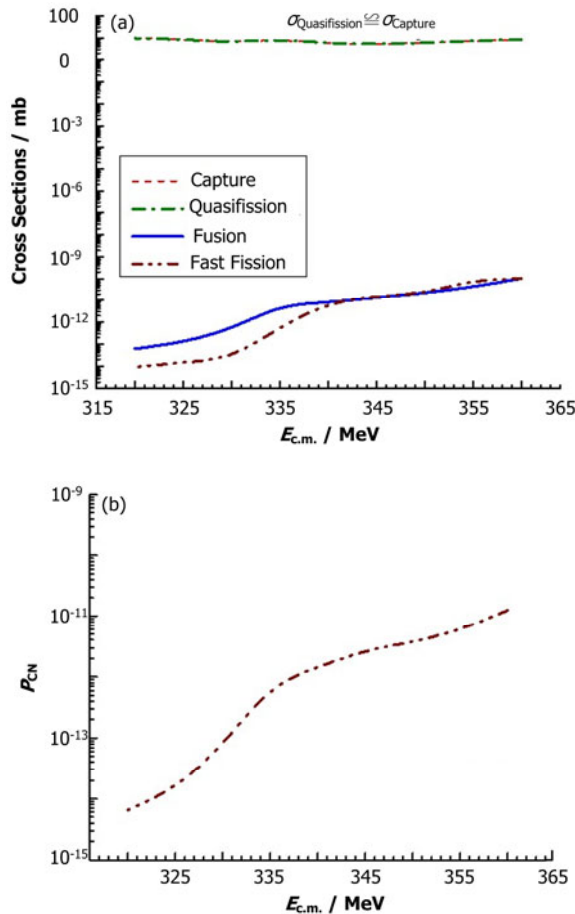


**Fig.3** (Color online) Capture, quasifission, fusion and fast fission cross sections (panel (a)), and the  $P_{\text{CN}}$  fusion probability (panel (b)), vs. the  $E_{\text{c.m.}}$  energy of the  $^{36}\text{Xe}+^{136}\text{Xe}$  reaction.

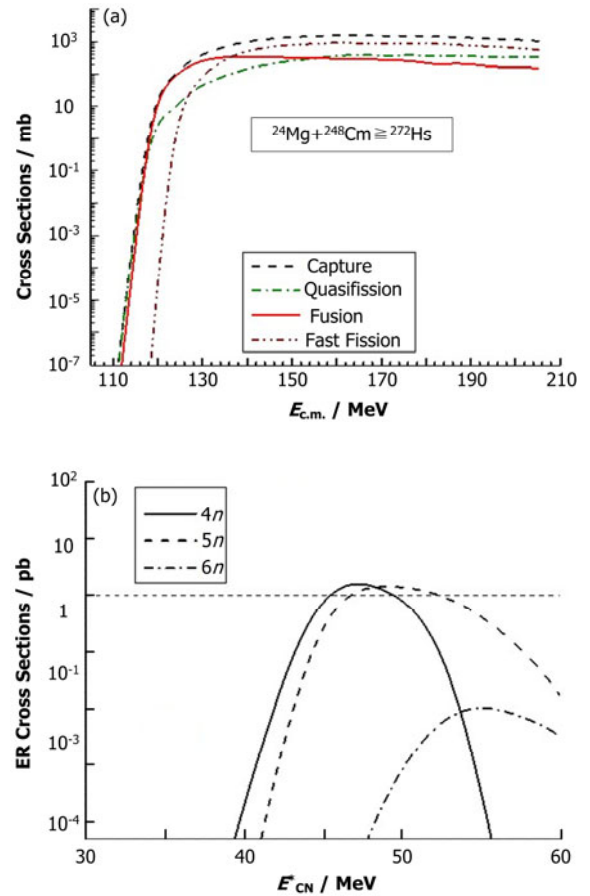


**Fig.4** (Color online) Capture, quasifission, fusion and fast fission cross sections (panel (a)) vs. the energy, and the individual evaporation residue cross sections (panel (b)) versus the  $E_{\text{CN}}^*$  excitation energy of CN, for the  $^{24}\text{Mg}+^{248}\text{Cm}$  reaction. In panel (b) the results of our calculation by using the masses and barriers of Refs.[17,18] are reported.

#### 4 Study on superheavy nuclei and perspectives for heavier superheavy elements

In order to estimate the realistic possibilities of synthesis of SHE by massive nuclei reactions, we performed calculations of the ER cross sections for set of reactions forming fissile compound nuclei with  $Z \geq 100$  at the same excitation energy ( $E_{\text{CN}}^* \sim 37$  MeV).

In Table 1, we present the set of elements by various entrance channels with different charge (mass) asymmetry parameters. It is interesting to observe and analyze the overall trend of the fusion probability  $P_{\text{CN}}$  and the evaporation residue yields for various reactions as a function of the charge  $Z_{\text{CN}}$  and of the parameter  $z=(Z_1 \times Z_2)/(A_1^{1/3} + A_2^{1/3})$  in order to draw some useful indications on the possible reactions leading to heavy nuclei with  $Z_{\text{CN}} \geq 100$  and particularly on reactions leading to SHE with  $Z_{\text{CN}} \geq 120$ . Fig.5 shows the fusion probability  $P_{\text{CN}}$  for the reactions

listed in Table 1 as a function of the charge  $Z_{CN}$  at excitation energy  $E_{CN}^* \sim 37$  MeV. As shown in Fig.5,  $P_{CN}$  slowly decreases with  $Z_{CN}$  but strongly decreases for more symmetric reactions in entrance channel leading to the same  $Z_{CN}$ . The trend of  $P_{CN}$  for the same investigated reactions appears more clear if we report the calculated  $P_{CN}$  as a function of the parameter  $z = (Z_1 \times Z_2) / (A_1^{1/3} + A_2^{1/3})$  representing the Coulomb barrier of interacting nuclei in the entrance channel if we divide this  $z$  parameter to the  $r_0$  nuclear parameter that is able to calculate the radius of each nucleus ( $R = r_0 A^{1/3}$ ) (see Fig.7 from Ref.[19]). In this last case, the values of  $P_{CN}$  reported at the given values of  $Z_{CN}$  (108, 118, 120, 122, 122, 124 and 126) represent different fusion probabilities for various entrance channels of reactions leading to the same  $Z_{CN}$ . The fusion probability  $P_{CN}$  strongly decreases by increasing the  $z$  parameter and by decreasing the charge (mass) asymmetry parameter of reactions in the entrance channel. The hindrance to fusion increases for more symmetric reactions and for higher Coulomb barriers of reactions in entrance channel. The evaporation residues after neutron emission only from the de-excitation cascade of CN can be observed for reactions with  $z$  parameter lower than the value of about 200. For reactions with values of  $z$  parameter included in the range about 200–235 the observation of residues is at limit (or it appears to be a very problematic task) of the current experimental possibilities. For reactions with  $z$  higher than 235 it is impossible to observe ER of CN after neutron emission only. We report in Table 2 that the results obtained for the investigated reactions leading to CN with  $Z=120, 122, 124$  and  $126$ , at  $E_{CN}^* \sim 37$  MeV.

**Table 1** Listed reactions are reported as a function of the charge  $Z_{CN}$  of CN (if it can be reached), and the parameter  $z = (Z_1 \times Z_2) / (A_1^{1/3} + A_2^{1/3})$  related to the Coulomb barrier of reacting nuclei in the entrance channel

Reactions	$Z_{CN}$	$z$	Reactions	$Z_{CN}$	$z$
$^{16}\text{O} + ^{238}\text{U}$	100	84	$^{86}\text{Kr} + ^{208}\text{Pb}$	118	286
$^{48}\text{Ca} + ^{208}\text{Pb}$	102	172	$^{132}\text{Sn} + ^{174}\text{Yb}$	120	328
$^{50}\text{Ti} + ^{208}\text{Pb}$	104	188	$^{64}\text{Ni} + ^{238}\text{U}$	120	253
$^{136}\text{Xe} + ^{136}\text{Xe}$	108	284	$^{58}\text{Fe} + ^{244}\text{Pu}$	120	242
$^{58}\text{Fe} + ^{208}\text{Pb}$	108	218	$^{54}\text{Cr} + ^{248}\text{Cm}$	120	229
$^{48}\text{Ca} + ^{226}\text{Ra}$	108	181	$^{132}\text{Sn} + ^{176}\text{Hf}$	122	337
$^{26}\text{Mg} + ^{248}\text{Cm}$	108	125	$^{54}\text{Cr} + ^{249}\text{Cf}$	122	234
$^{48}\text{Ca} + ^{243}\text{Am}$	115	193	$^{132}\text{Sn} + ^{186}\text{W}$	124	343
$^{48}\text{Ca} + ^{248}\text{Cm}$	116	194	$^{58}\text{Fe} + ^{249}\text{Cf}$	124	251
$^{48}\text{Ca} + ^{248}\text{Bk}$	117	196	$^{84}\text{Kr} + ^{232}\text{Th}$	126	307
$^{48}\text{Ca} + ^{249}\text{Cf}$	118	198	$^{64}\text{Ni} + ^{249}\text{Cf}$	126	267

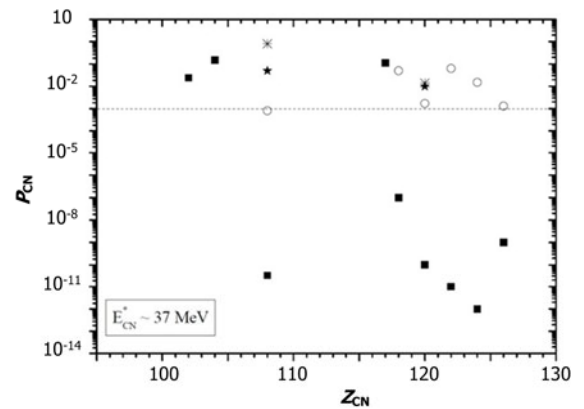


**Fig.5** Fusion probability  $P_{CN}$  calculated at the same excitation energy  $E_{CN}^* \sim 37$  MeV versus charge  $Z_{CN}$  for the reactions listed in Table 1. The different symbols (full squares, open circles, full stars and asterisks) are related to our calculated  $P_{CN}$  values in respect of the reactions listed in Table 1. The  $P_{CN}$  values are higher for higher mass asymmetric reactions.

**Table 2** Reactions leading to compound nuclei with  $Z_{CN}=120, 122, 124$  and  $126$ . As a function of the parameter  $z$  related to the Coulomb barrier in the entrance channel.  $\sigma_{ER}$  is the ER cross section after the neutron emission only from the de-excitation cascade of CN.  $P_{res/cap}$  is the ratio between the yields of evaporation residue  $\sigma_{ER}$  and the capture  $\sigma_{cap}$

Reactions	$Z_{CN}$	$z$	$\sigma_{ER} / \text{mb}$	$P_{res/cap}$
$^{54}\text{Cr} + ^{248}\text{Cm}$	120	229	$1.05 \times 10^{-10}$	$0.30 \times 10^{-11}$
$^{58}\text{Fe} + ^{244}\text{Pu}$	120	242	$5.40 \times 10^{-12}$	$1.70 \times 10^{-14}$
$^{64}\text{Ni} + ^{238}\text{U}$	120	253	$3.10 \times 10^{-15}$	$1.40 \times 10^{-16}$
$^{54}\text{Cr} + ^{249}\text{Cf}$	122	234	$1.40 \times 10^{-10}$	$1.30 \times 10^{-12}$
$^{58}\text{Fe} + ^{249}\text{Cf}$	124	251	$1.61 \times 10^{-15}$	$1.80 \times 10^{-17}$
$^{64}\text{Ni} + ^{249}\text{Cf}$	126	267	$4.40 \times 10^{-20}$	$6.50 \times 10^{-22}$

We estimated that only for the SHE with  $Z_{CN}=120$  it is possible to observe evaporation residues by reactions with  $z$  parameter lower than 230. The possibility of obtaining the heaviest  $^{302}119$  and  $^{305}120$  SHEs by using the  $^{48}\text{Ca}$  beam in the  $^{48}\text{Ca} + ^{254}\text{Es}$  and  $^{48}\text{Ca} + ^{257}\text{Fm}$  reactions, respectively, is restricted by difficulties in obtaining enough thick targets of  $^{254}\text{Es}$  and  $^{257}\text{Fm}$  because the other Es and Fm isotopes are radioactive with shorter lifetimes. Therefore, in order to reach heavier SHE, reactions with beams heavier than  $^{48}\text{Ca}$  (as for example  $^{50}\text{Ti}$ ,  $^{54}\text{Cr}$ ,  $^{58}\text{Fe}$ ,  $^{64}\text{Ni}$  and other heavier projectiles) against the above-mentioned actinide targets should be used. But, unfortunately, the evaporation residues cross sections strongly decrease by decreasing the charge (mass) asymmetry of reactants in the entrance channel.



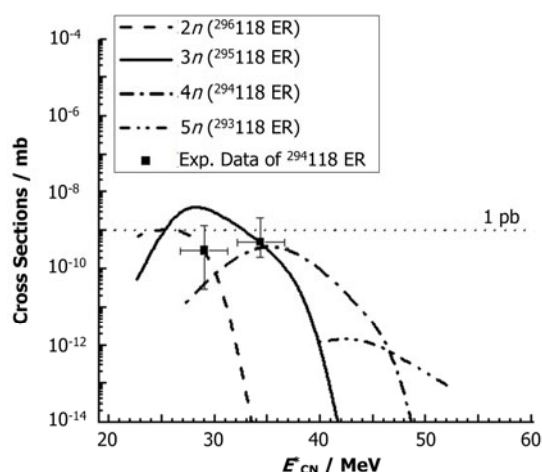


**Fig.6** Individual evaporation residue excitation functions after emission of 2 (dashed line), 3 (full line), 4 (dash-dotted line) and 5 (dash-double dotted line) neutrons from the  $^{297}118$  CN in the reaction of  $^{48}\text{Ca}+^{250}\text{Cf}$ . The experimental data (full squares) of the  $^{294}118$  ER formation cross section obtained from Ref.[5].

The first experiments which were performed at Flerov Laboratory of Nuclear Reaction of Joint Institute for Nuclear Reaction ( $^{58}\text{Fe}+^{244}\text{Pu}^{[20]}$ ) and at GSI of Darmstadt ( $^{64}\text{Ni}+^{238}\text{U}$  and  $^{54}\text{Cr}+^{248}\text{Cm}^{[21]}$ , and  $^{50}\text{Ti}+^{249}\text{Cf}^{[22]}$ ) to explore the synthesis of the  $Z=120$  SHE did not identify any event of the expected SHE. In our previous papers (Refs.[10,15]), we presented results of calculation about the above-mentioned reactions which could lead to the  $Z=120$  SHE, but we found values of the evaporation residue cross sections lower than 0.1 pb. Predictions of other authors are approximately near this value<sup>[23-27]</sup>. Therefore, it is necessary to improve the experimental conditions in order to be able to reach measurements of cross sections of the order of fb.

Moreover, we also studied four reactions induced by  $^{48}\text{Ca}$  on the  $^{249-252}\text{Cf}$  targets in order to analyze the effect of mass number and structure properties of nuclei in the entrance channel on the capture, quasifission, and complete fusion processes. The study and comparison of capture cross sections allows us to reveal the sensitivity of the model and results on the dynamical effects of the entrance channel (for results see Fig.1 of Ref.[28]), while the determination and analysis of the evaporation residue cross sections for the four reactions reveal the influence of the different structure of the formed  $^{297-300}118$  superheavy compound nuclei in the  $^{48}\text{Ca}+^{249-252}\text{Cf}$  reactions with different neutron rich

targets. In the following Figs.6 and 7, for example, the ER excitation functions obtained for the  $^{48}\text{Ca}+^{249,250}\text{Cf}$  reactions, respectively, by using the masses and barriers of Refs.[17,18]. We also investigated the formation of the heaviest evaporation residue nuclei from the  $^{299,300}118$  CNs which are formed in reactions induced by collision of the  $^{48}\text{Ca}$  projectiles with the heaviest accessible  $^{251,252}\text{Cf}$  actinide targets, and the results are comparable with the ones obtained for the reactions on the  $^{249,250}\text{Cf}$  targets.

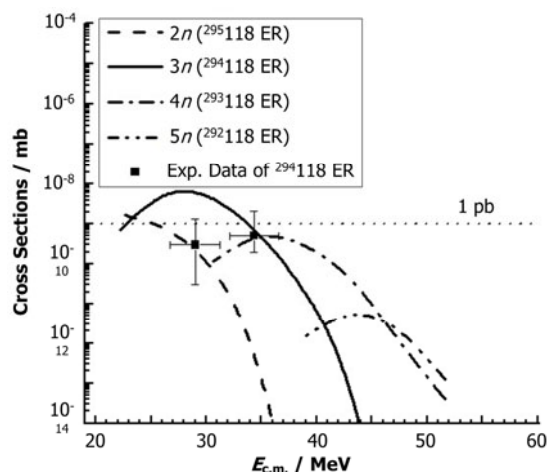


**Fig.7** As Fig.6, but for the  $^{48}\text{Ca}+^{249}\text{Cf}$  reaction.

By analyzing the 2, 3, 4 and 5 neutron emission channels along the de-excitation cascade of compound nuclei formed in the  $^{48}\text{Ca}+^{249,250}\text{Cf}$  reactions, we studied the possibilities of synthesizing the  $^{292-296}118$  ER nuclei. In addition, by considering the experimental conditions nowadays available in Laboratories, the more convenient and accessible reaction channels of observing evaporation residue nuclei are the 3 and 4 neutron emission channels in the  $^{48}\text{Ca}+^{249-252}\text{Cf}$  reactions at beam energies corresponding to the  $E_{\text{CN}}^*=25-40$  MeV interval. By comparing the results of our analysis regarding the study of the  $^{48}\text{Ca}+^{249,250}\text{Cf}$  reactions with the data obtained in the experiment of Ref.[5] regarding the observation of the  $^{294}118$  evaporation residue nucleus, we conclude that the better description of the experimental results is that the observed  $^{294}118$  synthesis events<sup>[5]</sup>, registered at two different beam energies, are contributed by the 3n-channel in the  $^{48}\text{Ca}+^{249}\text{Cf}$  reaction and 4n-channel in the  $^{48}\text{Ca}+^{250}\text{Cf}$  reaction, due to the inevitable presence of the  $^{250}\text{Cf}$  isotope in the  $^{249}\text{Cf}$  enriched target. Moreover, the

comparison of results obtained for the ER nuclei in the  $^{48}\text{Ca}+^{252}\text{Cf}$  studied reaction suggest the use of one target only constituted of all the Cf isotopes having longer lifetimes. This is more convenient either for the procedure of its preparation or in analysis of one experiment only. In fact, it is possible to observe and study a wide set of ER nuclei formed by  $2n$ ,  $3n$ ,  $4n$ , and  $5n$  emission channels, only changing the  $^{48}\text{Ca}$  beam energy  $E_{\text{lab}}$  in the range of 235–260 MeV.

## 5 Conclusion

At present time, it is a problematic task to measure ER cross sections of SHE with  $Z=120$ , and this is also impossible for reactions with  $z$  parameter higher than about 240. Then, mass symmetric reactions with  $z>240$ , as for example  $^{136}\text{Xe}+^{136}\text{Xe}$  reaction (where  $z=284$ ), cannot form ER nuclei because that reaction does not give sufficient fusion cross section. It is impossible to obtain SHE's with  $Z>120$  by complete fusion reactions since the  $z$  parameter is higher than 240. In reaction induced by  $^{48}\text{Ca}$  beam it is impossible to obtain ER nuclei higher than  $^{298}118$  by using Cf targets. Instead, by using a mixture of Cf isotopes as target, it is possible to explore by one experiment only the  $^{294-298}118$  ER cross sections in the 25–40 MeV excitation energy range. From the study of the present investigated systematics on reactions for the superheavy formations, we understand the role of the mass symmetry parameter of entrance channel on the fusion probability of reaction and evaporation residue yields. Regarding the results of the investigated reactions leading to the formation of compound nuclei with  $Z_{\text{CN}}=120, 122, 124$ , and  $126$  we affirm that it is still possible to reach and observe ER nuclei of the  $Z=120$  SHE by reactions with  $z$  parameter of about 230, while it is a very doubtful venture to synthesize the  $Z=122$  SHE by reactions with  $z$  parameter of about 234, or higher, by the current experimental resources and methods of observing evaporation residues. It appears out of every possibility to observe evaporation residue of SHE by reactions with  $z$  parameter in the entrance channel higher than 240. Therefore, it is impossible to form the  $Z=124$  and  $Z=126$  superheavy nuclei by the above-mentioned reactions. Consequently, it is an unrealizable dream to think of performing the  $^{132}\text{Sn}+^{208}\text{Pb}$  (with  $z=373$ ) and

$^{132}\text{Sn}+^{249}\text{Cf}$  (with  $z=431$ ) reactions in order to reach the  $^{340}132$  and  $^{381}148$  SHE, respectively, and by mass symmetric reactions like  $^{139,149}\text{La}+^{139,149}\text{La}$  (with  $z=317$  and  $306$ , respectively) in order to synthesize heavy and superheavy elements because of the absolute dominant contribution of the quasifission process after capture, and the fast fission process presents at stage of the already small probable formation of complete fusion.

## References

- 1 Fazio G, Giardina G, Mandaglio G, *et al.* Phys Rev C, 2005, **72**: 064614.
- 2 Fazio G, Giardina G, Lamberto A, *et al.* Eur Phys J A, 2004, **22**: 75–87.
- 3 Giardina G, Nasirov A K, Mandaglio G, *et al.* J Phys Conf Ser, 2011, **282**: 012006.
- 4 Nishio K, Hofmann S, Heßberger F P, *et al.* Phys Rev C, 2012, **82**: 024611.
- 5 Oganessian Y T, Utyonkov V K, Lobanov Y V, *et al.* Phys. Rev C, 2006, **74**: 044602.
- 6 Nasirov A K, Mandaglio G, Manganaro M, *et al.* Phys Lett B, 2010, **686**: 72–77.
- 7 Fazio G, Giardina G, Mandaglio G, *et al.* Mod Phys Lett A, 2005, **20**: 391–405.
- 8 Antonenko N A, Cherepanov E A, Nasirov A K, *et al.* Phys Rev C, 1995, **51**: 2635–2645.
- 9 Nasirov A K, Fukushima A, Toyoshima Y, *et al.* Nucl Phys A, 2005, **759**: 342–369.
- 10 Nasirov A K, Giardina G, Mandaglio G, *et al.* Phys Rev C, 2009, **79**: 024606.
- 11 Fazio G, Giardina G, Hanappe F, *et al.* J Phys Soc Jap, 2008, **77**: 124201.
- 12 D'Arrigo A, Giardina G, Herman M, *et al.* Phys Rev C, 1992, **46**: 1437–1444.
- 13 Giardina G, Hofmann S, Muminov A I, *et al.* Eur Phys J A, 2000, **8**: 205–216.
- 14 Sagaidak R N, Chepigin V I, Kabachenko A P, *et al.* J Phys G, 1998, **24**: 611–625.
- 15 Nasirov A K, Mandaglio G, Giardina G, *et al.* Phys Rev C, 2011, **84**: 044612.
- 16 Zhang H Q, Lin C J, Jia H M, *et al.* Phys Rev C, 2010, **81**: 034611.
- 17 Muntian I, Patyk Z, Sobbieczewski A. Phys Atom Nucl, 2003, **66**: 1015–1019.



- 18 Kowal M, Jachimowicz P, Sobiczewski A. *Phys Rev C*, 2010, **82**: 014303.
- 19 Mandaglio G, Nasirov A K, Curciarello F, *et al.* EPJ Web of Conferences, 2012, **38**: 01001.
- 20 Oganessian Y T, Utyonkov, V, Lobanov Y, *et al.* *Phys Rev C*, 2009, **79**: 024603.
- 21 Hofmann S, Heinz S, Ackermann D, *et al.* GSI Scientific Report No. PHN-NUSTATR-SHE-01, 2011, 205.
- 22 Düllmann Ch E, Yakushev A, Khuyagbaatar J, *et al.* GSI Scientific Report No. PHN-NUSTATR-SHE-02, 2011, 206.
- 23 Zagrebaev V I and Greiner W. *Nucl Phys A*, 2007, **787**: 363–372.
- 24 Liu Z H and Bao J D. *Phys Rev C*, 2009, **80**: 054608.
- 25 Adamian G G, Antonenko N V, Scheid W. *Eur Phys J A*, 2009, **41**: 235–241.
- 26 Siwek-Wilczynska K, Cap T, Wilczynski J. *Int J Mod Phys E*, 2010, **19**: 500–507.
- 27 Nan Wang, Zhao E G, Scheid W, *et al.* *Phys Rev C*, 2012, **85**: 041601R.
- 28 Mandaglio G, Giardina G, Nasirov A K, *et al.* *Phys Rev C*, 2012, **86**: 064607.